Switchable phase transition of crystalline to amorphous state of potassium nitrate single crystal

A. Siva Kumar, P. Eniya, S. Sahaya Jude Dhas, Abdulrahman I. Almansour, Raju Suresh Kumar, Natarajan Arumugam, J. Kalyana Sundar, Shubhadip Chakraborty, S. A. Martin Britto Dhas

Switchable Phase Transition of Crystalline to Amorphous State of Potassium Nitrate Single Crystal

A.Sivakumar[1], P.Eniya[2], S.Sahaya Jude Dhas[3], Abdulrahman I.Almansour[4], Raju Suresh Kumar[4], Natarajan Arumugam[4], J.Kalyana Sundar[2], Shubhadip Chakraborty[5], S.A.Martin Britto Dhas[1]*

[1]Shock Wave Research Laboratory, Department of Physics, Abdul Kalam Research Center, Sacred Heart College, Tirupattur, Tamil Nadu, India – 635 601

[2]Department of Physics, Periyar University, Salem, 636011, Tamil Nadu, India

[3]Department of Physics, Kings Engineering College, Sriperumbudur, Chennai, Tamilnadu, India - 602 117

[4]Department of Chemistry, College of Science, King Saud University, P.O. Box 2455, Riyadh, Saudi Arabia- 11451

[5]Institut de Physique de Rennes, UMR CNRS 6251, Université de Rennes 1, 35042 Rennes Cedex, France

Corresponding Author: martinbritto@shctpt.edu

Abstract

High-pressure materials science always has a special benchmark in the current research areas wherein dynamic shock waves have also made striking inroads on a par with high-pressure experiments in solids and have marked a tremendous impact in expanding the materials science research both in academics as well as applications point of view. In this context, we report and demonstrate the switchable phase transition of crystalline to the amorphous state of potassium nitrate (KNO_3) single crystal at shocked conditions such that the observed results of phase transition have been evaluated by X-ray diffraction (XRD), Raman and optical spectroscopic as well as Field –emission scanning electron microscopic (FE-SEM) techniques. The observed phase transition sequence is crystal-crystal-crystal-amorphous-crystal-glassy crystalline nature that is exhibited by KNO_3 crystals with respect to 0, 1, 2, 3, 4, and 5 shock pulses. The formation of amorphous KNO_3 is because of the rotational disorder of the oxy-anions of the NO_3 units and the positional disorder of potassium ions. Strikingly, to date, it could be the first report of amorphization on KNO_3 considering both the static pressure and temperature experiments. Due to the ability of potential switching between crystalline and amorphous states, the title material is a good fit for the applications of optical data storage and molecular switching.

Key-words: Shock waves, KNO_3 crystal, Rotational disorder, Switchable phase transition

Introduction

Surfing through the literature, to date, materials of switchable phase transition are always in the midst of top-class essentials which are now gaining momentum as these materials are tagged to be the latest benchmark for the modern industries. The pooled experimental results that have been obtained over the years have the potential paradigm to unleash the mechanisms such that the fallout could be entrenching. The resounding success of switchable phase transition materials attracts a tall order demand in the electronic industry as they can fit into several kinds of applications such as molecular switches, optical data storage, sensor, phase shifter and transmitters [1-5]. As far as it is known, to find the switchable phase transition materials by the impact of pressure through the experimental techniques can be classified into two general categories: in-situ[6-8] and ex-situ [9,10] experiments, respectively. Most of the in-situ experiments have been carried out by diamond anvil cell (DAC) technique with which it has been found that most of the

materials obey the switchable phase transition during the compression and decompression wherein several transitions are crystal – crystal [11,12] and crystal – amorphous [13,14] whereas the process of switchable phase transition remains to be highly unusual. Moreover, a few of the materials undergo the irreversible phase transition during the decompression [15,16]. It could be noted that, in the case of in-situ experiments, the properties of materials are probed while the test specimen is subjected to compression such that a new phase emerges and when it is decompressed it comes back to its original ambient phase. Hence, if the materials possess interesting functional properties at high-pressure regimes, such properties could not be retained by the materials after coming back to the ambient conditions [11-14]. Dynamic shock wave loaded conditions are usually referred to as an ex-situ experimental type for which a considerable amount of research has been documented in the articles of solid-state sciences over the years and until now [17,18]. In the case of materials, while subjected to the dynamic shock wave loaded conditions, a variety of changes such as crystallographic phase changes [19,20], magnetic state changes[21-23], molecular phase changes [23] have been observed which in general significantly lead to changes in their functional properties. Interestingly, in most of the cases, such shock wave induced phase transitions occurring on solids do not revert while coming back to the ambient conditions. According to the literature reports, shock wave-induced irreversible phase transition of solids is quite known compared to the reversible phase transition occurring in both bulk and nanocrystalline materials. The concept of shock wave-induced reversible phase transition and its mechanism still remain to be in the dark such that a very few reports only have been documented in this topic to date [24]. Switchable crystallographic phase transition has been documented on K_2SO_4 (β-α-β) crystals with respect to the number of shock pulses such as 0, 1, and 2 pulses, respectively by Sivakumar et al [24] who have also achieved a couple of magnetically switchable phase transitions in technologically potential nanocrystalline materials such as Co_3O_4 [21], α-MnO_2 [22], and $ZnFe_2O_4$ [23].

In the present study, we have chosen potassium nitrate single crystal for the shock wave-induced phase change analysis which is one of the standard reference materials being used in the thermal analysis [25,26]. Many researchers have examined the phase stability by performing experimental analysis at static high-pressure and high-temperature conditions and found several interesting results [25-28]. From the crystallographic point of view, the title crystal has three major crystal structures that are phase-II (α-KNO_3- Pmcn), phase-I (β-KNO_3- R3m) and phase - III (γ-

KNO_3-R3m) and a few more high-pressure phases are known [28]. At ambient temperature, the test sample is crystallized in the Pmcn space group which is denoted as phase - II (α-KNO_3). While heating the phase–II KNO_3 at 129° C, it is transformed to the phase-I (β-KNO_3) and again cooling at 123° C, it undergoes to the phase-III which on further cooling at 115° C, comes back to the phase-II [28]. The lattice parameters of the phase-II are a = 5.414 Å, b = 9.164 Å and c = 6.431 Å which belongs to the aragonite crystal structure. The lattice constants of phase-I are a = 5.425 Å and c = 9.836 Å while phase –III have the respective values a = 5.487 Å and c = 9.156 Å such that both the crystals possess the calcite type crystal structure. From the crystallographic point of view, phase-I and phase-III are almost similar while all the three crystal structures are found to be highly sensitive to high-pressure and high-temperature. A considerable amount of research has been documented which is based on the heating and cooling wherein it has been found the above-mentioned phase-II-I-III-II such that the reversible phase transitions occurring at different temperatures are considered as major key points to achieve the successful completion of reversible phase transitions [29-32]. From the high-pressure point of view, Iqbal et al., have demonstrated the pressure-induced phase-II to phase-IV (Pnma) phase transition in KNO_3 at 3.2 kbar and during the decompression, phase II has been observed at 0.2 kbar [29]. Teng et al have performed the pressure compression experiment and found phase-II — phase-III transition at 800 bars [30]. Worlton et al have found the phase KNO_3-IV that is the orthorhombic Pnma with a = 7.4867 Å, b = 5.5648 Å, and c = 6.7629 Å at 3.6 kbar [31]. Such kind of high-pressure and high-temperature experiments on KNO_3 may provide some general understanding of the structural phase transition concepts which are closely associated with the rotational disordering of anion groups in ionic molecular solids. The successive phase transformation studies on KNO_3 continue to be the subject of intense research activity for several decades. Shock wave also triggers the rotational disorder – order phase transition in ionic solids [24]. Hence in the present experimental investigation, a few interesting structural results could be expected.

On those lines, we present the switchable phase transition occurring between crystalline and amorphous states at shocked conditions and the results have been screened by diffraction and spectroscopic techniques. As of now, from the literature survey, amorphization of KNO_3 is not yet reported.

Experimental section

Pure potassium nitrate compound (99% purity) was purchased from the Sigma-Aldrich Company and the slow evaporation technique was utilized to grow required bulk size crystals such that optically good quality single crystals were obtained for the present investigation. Briefly, 50ml volume of deionized water was taken in a beaker wherein potassium nitrate was added slowly till the saturation was achieved. Thereafter, the potassium nitrate solution was stirred constantly for the next five hours using a magnetic stirrer to obtain a highly homogeneous solution. After the completion of the stirring process, the solution was filtered and kept separately in a dust-free environment without any external disturbance so as to enable crystallization at room temperature. After 30 days, optically transparent crystals have been harvested and utilized for the shock experiments. Before shock wave loadings, the test samples of same the dimension have been cut and well-polished using polishing sheet and performed the shock wave recovery experiment. The working mechanism of the shock tube [32] and the procedure of shock wave loading on the crystals have been discussed in our previous articles [33] and the details of the shock wave loading procedure is provided in the supplementary section. For the present experiment, we have chosen totally six optically transparent single crystals of equal dimensions ($5\times5\times1$ mm^3) possessing the same (110) crystallographic plane. Among the six KNO_3crystals, one crystal has been kept as the control crystal while the remaining five crystals have been used for shock wave impact studies. In the present experiment, we have used shock waves of Mach number 1.7 with which the five crystals have been treated by shock waves of the order of 0, 1, 2, 3, 4 and 5 counts, respectively. One shock pulse has the transient pressure and temperature of 1.0 MPa and 644 K, respectively. After the completion of the shock wave loading procedure, the crystals have been sent for analytical studies such as XRD, Raman and UV- DRS spectral analyses. Note that we have carried out the above-mentioned analyses for the single crystals of KNO_3.

Results and Discussion

X-ray Diffraction

Powder X-ray diffractometry (Rigaku – SmartLab X-ray Diffractometer, Japan) has been adopted to examine the crystallographic phase changes of the title crystal and the obtained XRD patterns of the control and shocked crystal are presented in Fig.1 and the comparison is made with the standard simulated XRD pattern of CIF number ICSD: 10289 (Pmcn: phase-II) and JCDPS card number 05-0377 [25]. The obtained XRD peaks of the control are found to be well-matched

with the room-temperature phase (Pmcn) of α-KNO_3 crystal. While looking at the diffraction angle from 10-80°, the control sample has two prominent diffraction peaks at 19.4° and 19.7° degrees which belong to (110) and (020) planes, respectively and the corresponding zoomed-in version of the XRD patterns are portrayed in Fig.2. It could be noted that the chosen unidirectional rectangular single crystal should have ideally exhibited only one diffraction peak whereas here we have observed four diffraction peaks ((110), (020), (200) and (231) for the control crystal. According to the morphology of the title crystal, (110) and (020) planes are very closets of rectangular shape facets [34] and hence, it is quite difficult to cut single oriented crystal along (110) plane. As seen in Fig.2, the (110) plane has a quite lower crystallinity than that of the (020) which clearly demonstrates that the (110) plane has quite a high degree of structural disorder and such disordered crystals are quite common in the crystal growth of slow evaporation technique because of the uneven evaporation process [35,36].

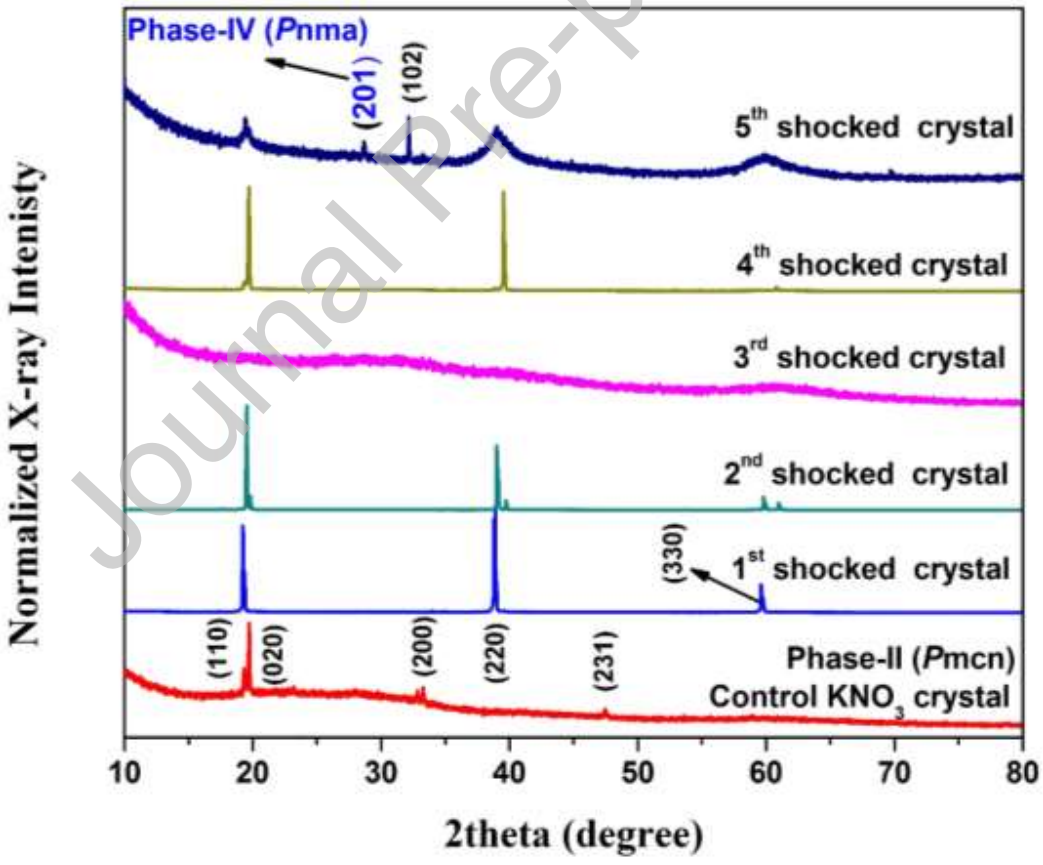

Fig.1 XRD patterns of the control and shocked KNO_3 crystals

At the first shocked condition, significant changes have been observed and the corresponding XRD patterns are portrayed in Fig.1 and Fig.2 in which the (110) plane has gained X-ray intensity. The appearance of the corresponding higher-order diffraction peaks located at 38.9 ° and 59.5 ° belong to the (220) and (330) planes, respectively. The increment of the diffraction peak intensity and the formation of higher-order diffraction peaks clearly indicate that the net degree of crystalline nature is significantly increased at the 1st shocked condition. On the other hand, (020) plane has completely disappeared at the1st shocked conditions that may be due to the re-orientational effect of the diffraction planes enforced by the shock waves and similar results have been observed in potassium dihydrogen phosphate [37]. At this stage, structural defects and rotational disorder of the NO_3 ions could have happened at the shocked condition. As mentioned already, the control crystal has a slight disorder in the crystal packing that could be reduced by static re-crystallization and dynamic re-crystallization [38, 39,40].

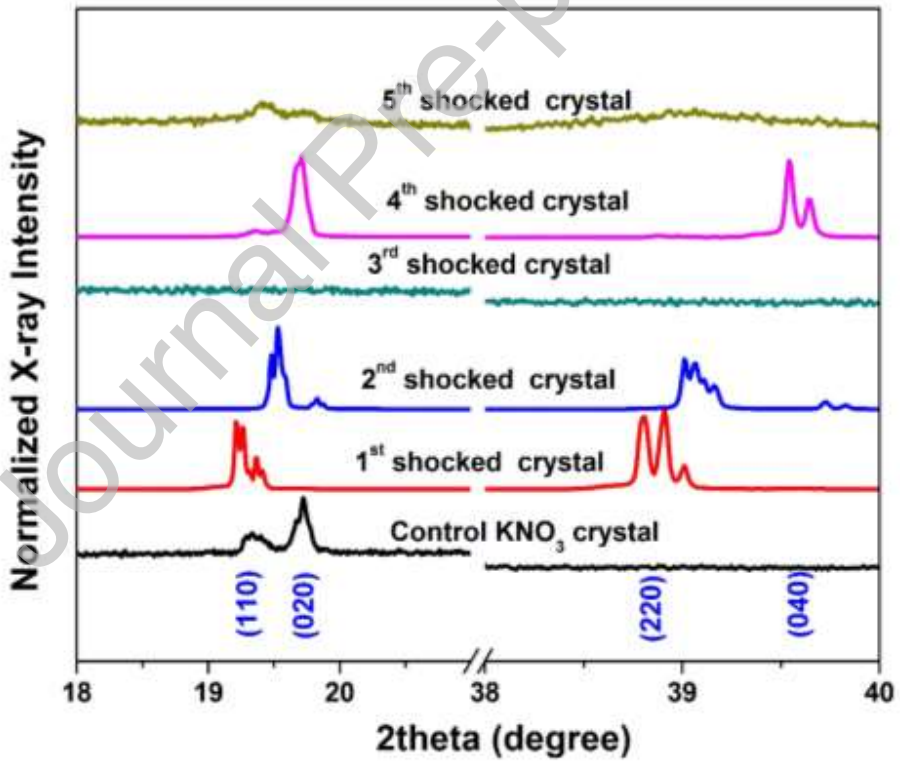

Fig.2 Zoomed-in version of the XRD patterns of the control and shocked KNO_3 crystals

At the first shocked condition, there is no high-temperature phase (β-KNO_3) observed. The (110) and its higher generation diffraction peak (220) are retained at the second shocked condition. In addition to that, a slight signature can be seen for the (020) plane and the corresponding diffraction patterns are presented in Fig.1 and Fig.2. The observed appearance and disappearance of the diffraction planes may be associated with the NO_3 network and their orientation [29-31]. At shocked conditions, the NO_3 network and their orientation may change with respect to the number of shock pulses and as a result, changes are observed in the diffraction pattern. As seen in Fig.2, the higher angle diffraction peak (220) is highly distorted and hence the degree of crystallinity might have been reduced. At the 2nd shocked condition also, no crystallographic phase transition is observed. At the 3rd shocked condition, none of the crystalline peaks is visible even in the zoomed-in version of the XRD patterns and hence the complete phase transition of crystal to amorphous nature is observed. The occurrence of the amorphization may be due to the existence of the positional disorder of the potassium ions and rotational anionic disorder of the NO_3 units. From the crystallographic point of view, phase-II KNO_3 crystal belongs to the aragonite type crystal structure wherein the anion and cation units are highly sensitive for the high-temperature and high-pressure and their results have been well documented [29-31].

While increasing the number of shock pulses, the net transient pressure is increased and it may be able to sustain after the critical pressure regime such that the test crystal may undergo the direct transition to the amorphous phase without going through any intermediate phases. At this stage, the actual lattice positions of the potassium ions and NO_3 ions are significantly altered and the schematic diagram of the atomic positions of the crystalline and amorphous nature of the KNO_3 crystals is depicted in Fig.3. As per the crystal structure of the phase-II of KNO_3 (Fig.3a), the NO_3 units are almost in a perfect triangular shape and the NO_3 ions do not lie exactly midway between two adjacent K^+ planes but are slightly displaced in the c direction. As we increase the number of shock pulses, the nitrogen atom deviates largely along the c-axis from the coplanar arrangement of the nitrogen and oxygen atoms within each NO_3 ion [41,42]. In such a case, the crystal symmetry of Pmcn may collapse resulting in the formation of an amorphous phase. It could be noted that the formation of the amorphous phase is purely due to the topological disorder of the K and NO_3 groups and not from the intra-bond breakage of the anions and cations [24]. But slight changes can be seen in the angle of the N and O atoms in the case of the amorphous phase. As seen in Fig.3b, the crystalline phase-II of KNO_3 has the perfect triangular shape of arrangement of oxygen atoms

around the nitrogen atoms. But in the case of the amorphous phase, the triangular shape is destroyed such that the bond distance between N and O atoms might have also changed with the K atom's displacement. In this context, the crystal symmetry may break and induce the formation of the amorphous state of KNO_3.

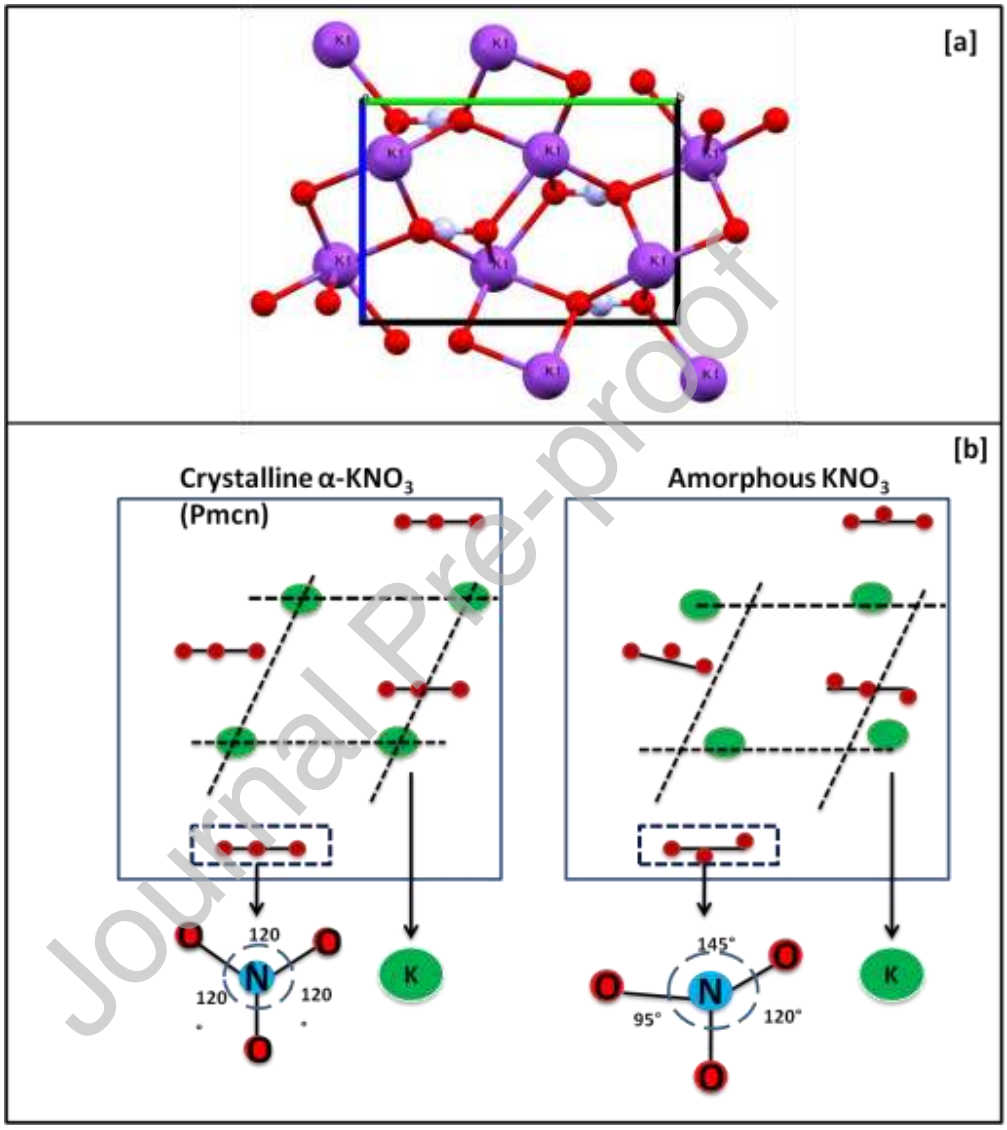

Fig.3 (a) crystal packing of phase-II of KNO_3 (b) Schematic diagram of the possible mechanism of the transition of crystal to amorphous nature of phase –II KNO_3

Surprisingly, at the 4th shocked condition, the phase transition of amorphous to the crystalline state is observed which belongs to the phase-II (Pmcn) crystal structure. At the 4th

shocked conditions, the existence of the positional disorder and rotational disorder of the cation and anion groups in the amorphous phase may turn into the disorder- order process of NO_3 which might lead to the occurrence of the phase-II. In a similar manner, disorder K_2SO_4 (β-phase) crystal is phase transformed to the order-K_2SO_4 (α-phase) at shocked conditions [24]. At the 5^{th}shocked condition, phase-II of KNO_3 crystal is again observed along with a very small amount of phase-IV (ICSD: 85491- Pnma) but with very poor crystalline nature and hence it is considered as a glassy-crystalline nature of phase-II and the phase diagram of the title crystal with respect to the number of shock pulses is depicted in Fig.4. At the 5^{th} shocked condition, the title crystal might have experienced considerable rotational disorder of the NO_3 units mainly about their triad axes and positional disorder of the K atoms resulting in the observed glassy-crystalline phase-II of KNO_3. It could be noted that the existence of two phases such as crystal and glassy-crystalline simultaneously at the 5^{th} shocked condition may be due to the thermal history of the crystal. Furthermore, in the case of the phase-II, c-axis is loosely packed such that, while temperature and pressure are increased at shocked conditions, a large thermal expansion and compression might appear resulting in a significant restriction on the rotational motion of the NO_3 units that enforce significant structural phase transitions with respect to the number of shock pulses.

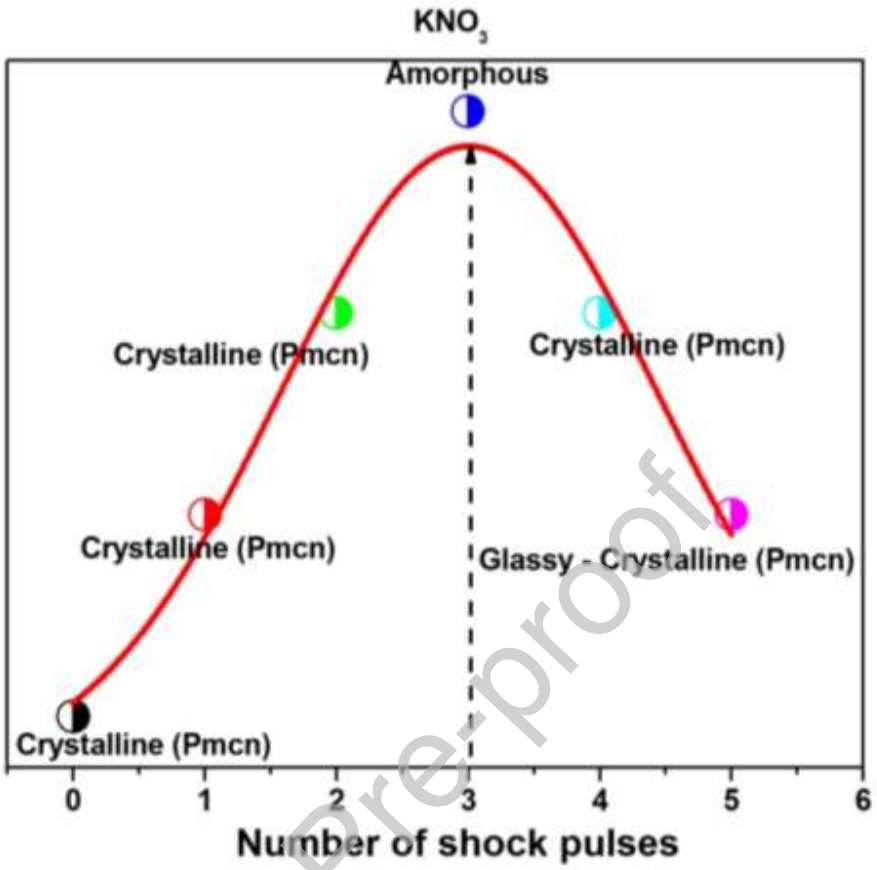

Fig.4 Phase diagram of the phase-II KNO_3 crystal with respect to the number of shock pulses

Raman Spectroscopic Results

Furthermore, Raman spectroscopic measurements have been carried out for the control and shocked crystal so as to ensure the phase transitions of the title crystal with respect to the number of shock pulses as that of the phase diagram presented in Fig.4. In addition to that, Raman spectroscopic results can clearly demonstrate the rotational order–disorder of the NO_3 ions at shocked conditions and based on the XRD discussion, the concept of the rotational disorder-order of the NO_3 ion groups have the major contribution of enforcing the amorphization and glassy-crystalline nature of the title crystal at shocked conditions. Hence, Raman spectroscopic analysis is highly required to make a solid conclusion on the observed XRD results. Hence, we have performed the Raman measurements for the range 50-1500 cm^{-1} and the obtained Raman spectra are presented in Fig.5.

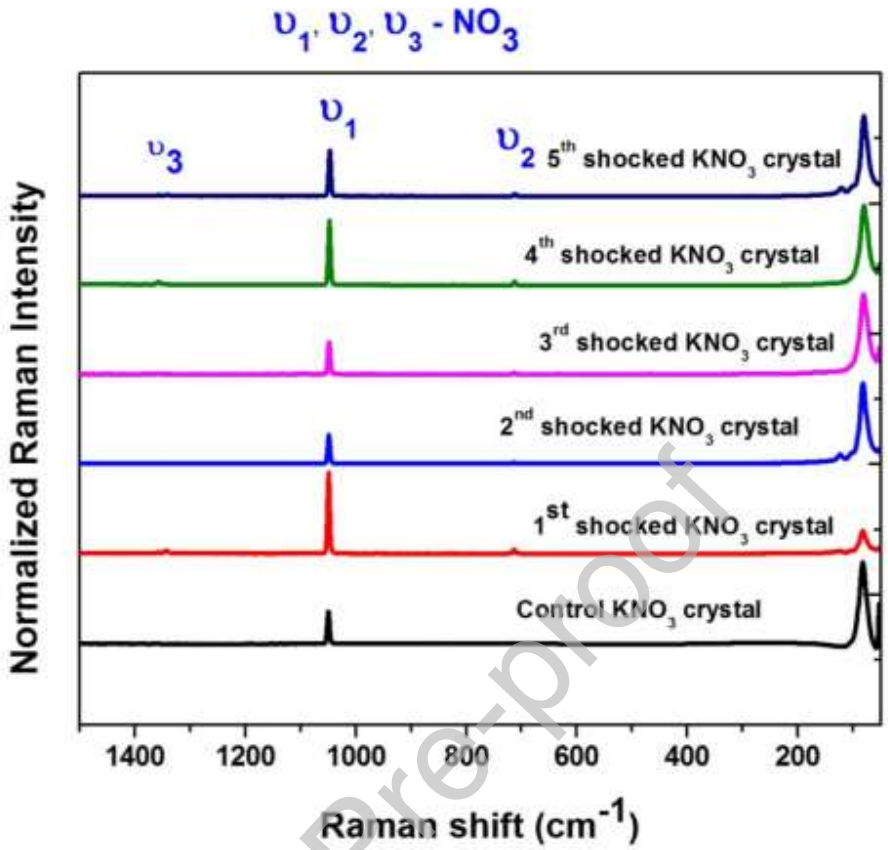

Fig.5 Raman spectra of the control and shocked KNO_3 crystals

Based on the previous reports, the phase-II of KNO_3 crystal should have NO_3 vibrational Raman bands at 1354 cm^{-1}(υ_3-NO_3), 1341 cm^{-1}(υ_3-NO_3), 1042 cm^{-1}(υ_1-NO_3), and 703 cm^{-1}(υ_2-NO_3), respectively [43]. As seen in Fig.5, the control sample has only one internal Raman band of υ_1-NO_3 at 1045 cm^{-1} whereas υ_3-NO_3 and υ_2-NO_3 Raman bands are not clearly visible which may be due to the occurrence of the lattice defects and structural disorder during the crystal growth. At the first shocked condition, the above-mentioned distinct vibrational Raman bands such as υ_2, υ_1, and υ_3-NO_3 bands are located at 712, 1051, 1342, 1358 cm^{-1} and the observed Raman band positions are found to be well-matched with the phase-II of KNO_3 crystal [43] which is consistent with the XRD results. During the 1st shocked condition, the grown crystal's disorder is significantly reduced and hence the υ_2, and υ_3-NO_3 Raman bands have gained a significant improvement in intensity as appearing appropriately in the respective Raman band positions. In addition to that, based on the above-motioned three vibrational Raman bands of NO_3, υ_3- region, Raman bands of NO_3 only have a greater contribution as compared to the other two NO_3 Raman bands on the enforcement of the

phase transitions of KNO_3 [43,44]. Hence, it is presented the zoomed-in version of the υ_3- region NO_3 Raman bands of the control and shocked KNO_3 crystals in Fig.6 wherein the doublet Raman bands are clearly visible so that the formation of phase-II is confirmed at the 1st shocked condition [43]. At the 2nd shocked condition, υ_2-NO_3, υ_1-NO_3 and υ_3-NO_3 Raman bands are located at 714, 1048, 1342, and 1359 cm^{-1}, respectively and the observed Raman spectrum is portrayed in Fig.5. Based on the observed Raman band positions, the intense characteristic Raman band of υ_1-NO_3 experiences a lower frequency shift that may be due to the existence of the lattice disorder and rotational disorder of the NO_3 groups at the 2nd shocked condition. In addition to that, υ_3-NO_3 doublet Raman bands are retained at the same Raman positions at the 2nd shocked condition wherein the normalized Raman intensity is significantly reduced such that this Raman band region also supports the existence of disorder in KNO_3 crystal.

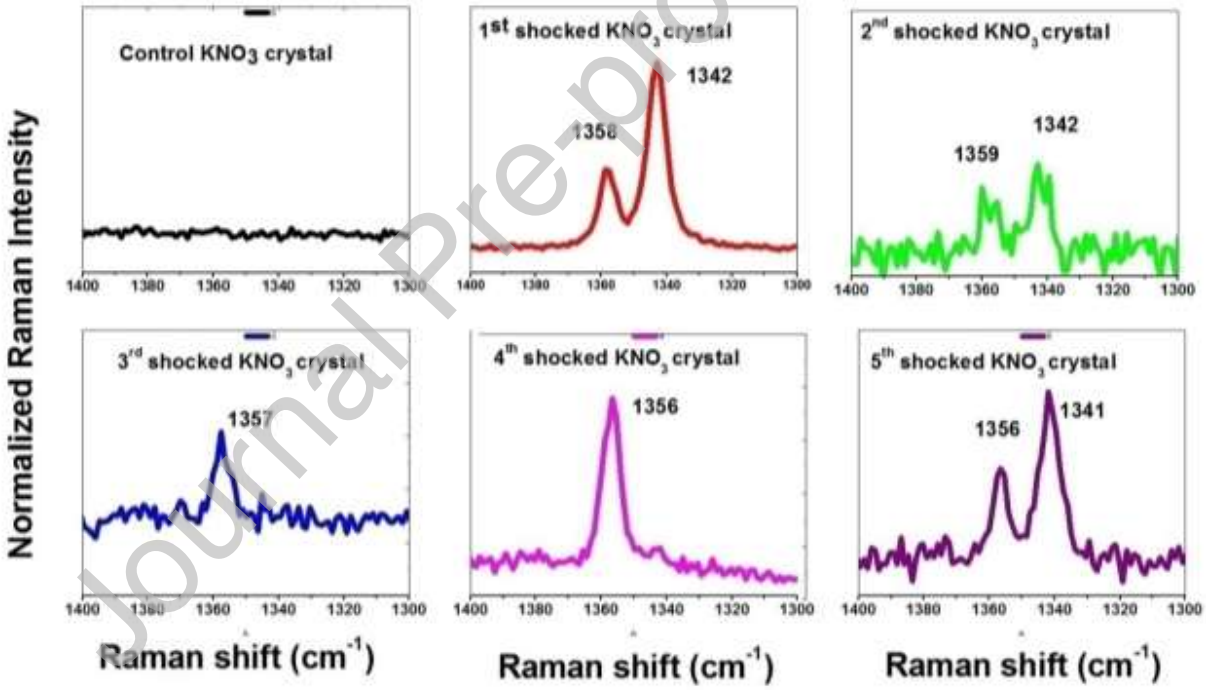

Fig.6 Zoomed-in versions of υ_3-NO_3Raman bands of the control and shocked KNO_3 crystals

At the 3rd shocked condition, υ_2-NO_3, υ_1-NO_3 and υ_3-NO_3 Raman bands are located at 713, 1047 and 1357 cm^{-1}, respectively and the observed Raman spectrum is depicted in Fig.5. As seen in Fig.6, the doublet Raman band is converted as a singlet Raman band that is located at 1357 cm^{-1} and as per the XRD results, the disappearance of the lower frequency Raman band of NO_3 may

be due to the formation of the amorphous phase of KNO_3. At the 4th shocked condition, υ_2-NO_3 υ_1-NO_3 and υ_3-NO_3 Raman bands are located at 714, 1051 and 1356 cm^{-1}, respectively. It could be noted that, while compared to the 3rd shocked υ_1-NO_3 Raman band position, the 4th shocked Raman band position has gained a higher frequency shift that indicates the phase transition wherein the normalized intensity has also increased. This clearly shows amorphous to the crystalline phase transition due to the rotational disorder-order of NO_3 ions based on the dynamic re-crystallization. On the other hand, as seen in Fig.6, the υ_3-NO_3 doublet Raman band is converted as singlet Raman band with higher intensity located at 1357 cm^{-1} whereas the lower frequency Raman band has very less intensity. At the 5th shocked condition, υ_2-NO_3, υ_1-NO_3 and υ_3-NO_3 Raman bands are located at 710, 1046, 1342 and 1356 cm^{-1}, respectively. Based on the observed Raman band positions, like that of 3rd shocked conditions, υ_2-NO_3,υ_1-NO_3 Raman bands are shifted towards the lower frequency region which may be due to the occurrence of rotational and positional disorder of the NO_3 ions. In Fig.6, the υ_3-NO_3 Raman band region shows a couple of humps in the single Raman band especially in the lower frequency region of the NO_3 Raman band. This may be due to the presence of disorder in the crystal system. Raman spectral results also provide strong evidence for the formation of the amorphous KNO_3 that also supports the XRD results with respect to the number of shock pulses. More importantly, continuous changes observed in the υ_3-NO_3 Raman band region with respect to the number of shock pulses show that the test sample is highly sensitive to the shock transient pressure and temperature.

Optical Spectroscopic Results

Followed by the diffraction and vibrational spectroscopic measurements, electronic spectral analysis has been carried out to understand better the inter-bond pattern changes of the control and shocked KNO_3 crystals. Hence, optical transmittance has been performed on the control and shocked crystals over the wavelength region between 200 and 800 nm using a UV-DRS- Shimadzu- UV-3600 plus spectrometer and the obtained optical transmittance patterns are presented in Fig.7. As seen in Fig.7, the control sample has the primary strong dichroism absorption band at 264 nm which is the characteristic electronic bond pattern of the NO_3 groups present in the title crystal such that the observed optical transmittance is found to be well-matched with the previous reports [45]. Furthermore, a few absorption bands are located at 369, 405, 472,

577 and 665 nm which may be due to the contribution of secondary dichroism absorption bands of the title crystal [46].

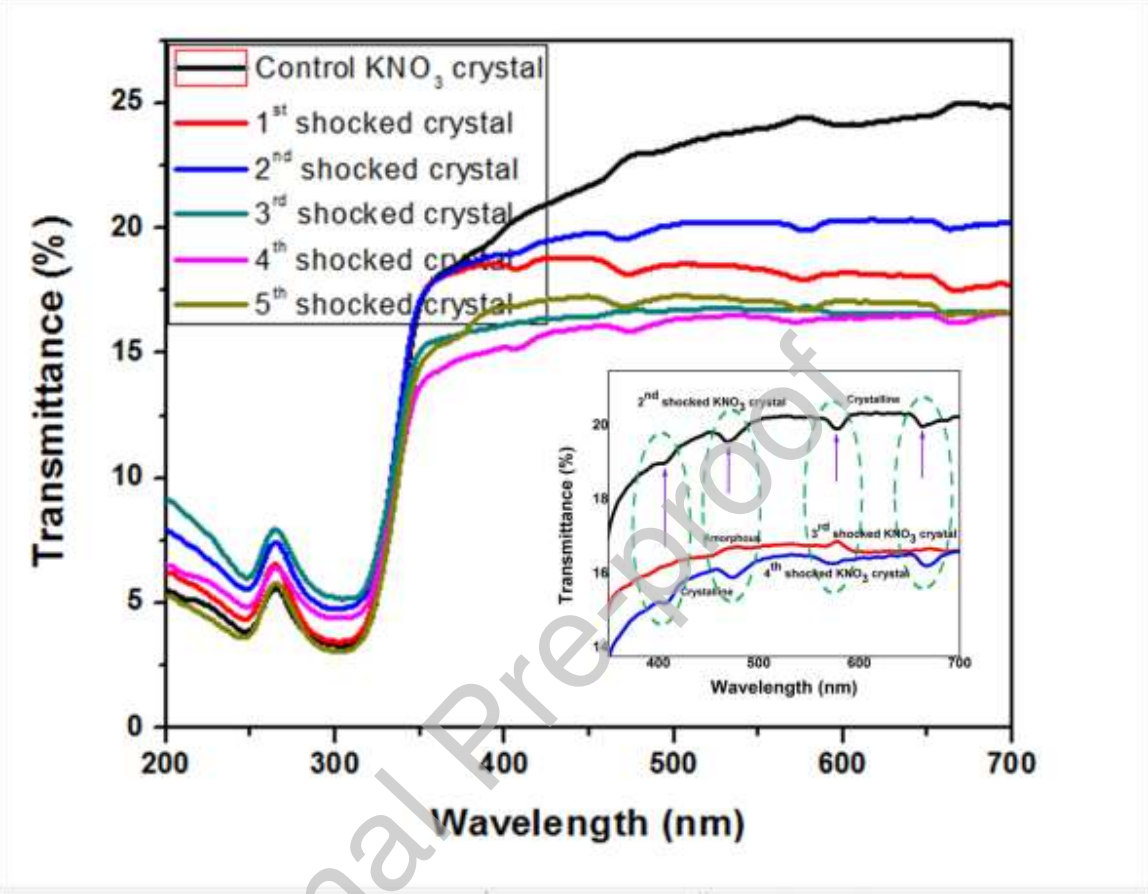

Fig.7 Optical transmittance spectra of the control and shocked KNO_3 crystals

On the one hand, at shocked conditions, there are no significant changes such as absorption band edge and band shifts observed in the primary NO_3 absorption band region with respect to the number of shock pulses. On the other hand, noticeable changes are visible particularly at the region of crystal-amorphous–crystal switchable phase transitions. Except at the 3rd shocked condition, all the optical transmission spectra have retained the primary and secondary NO_3 absorption band edges with very fine changes that clearly demonstrate the maintenance of the phase-II at 1st, 2nd, 4th and 5th shocked conditions. It could be noted that, from an optical spectroscopic point of view, drastic changes could not be seen even in the transition of phase-II (Pmcn) to phase-I (R3m) phases [45]. For a better understanding of the crystal-amorphous–crystal phase transition observed at 2nd, 3rd and 4th shocked conditions, it is presented the respective optical transmission spectra as an

insert in Fig.7. Moreover, the above-mentioned parameters have led to significant changes in the absorption energy bands of the electronic system based on the degree of lattice disorder [47,48]. As per the above-mentioned references and as seen in Fig.7, the 2nd shocked crystal has the secondary NO_3 absorption bands that disappear at the 3rd shocked condition and re-appear at the 4th shocked condition which may be the possible reason for the switchable crystal to the amorphous states of KNO_3 crystal at shocked condition. As discussed in the XRD and Raman analyses, at the state of amorphization in KNO_3, a significant positional and rotational disorder of the NO_3 groups and the positional disorder of the K atoms have occurred at which such cases significantly affect the conduction of the electrons from the ground state to excited state that is induced by the absence of a few absorption bands of the NO_3 bands and similar kind of results have been reported in antimony trisulphide thin films [47,48]. The significant rotational and positional disorder of the NO_3 groups might have interrupted the n -$\pi*$ transition resulting in the absence of corresponding absorption bands in the amorphous phase of KNO_3. Finally, it is clear that the intra-molecular electronic transitions of NO_3 have significantly changed at the 3rd shocked condition and induced the electronic disorder of the sample such that the resultant effect has enforced the amorphous nature.

Surface morphological Analysis

Field emission scanning electron microscopic (FE-SEM) imaging technique has been adopted to ensure the surface morphological changes of the control and shocked KNO_3 samples. The obtained micrographs are presented in Fig.8 wherein the control sample has a flat surface and the presence of slender line defects that are quite visible at the top surface of the crystal may be due to the formation of defects during the crystal growth. In the case of crystal growth achieved by the slow evaporation technique, such kinds of defects are uncontrollable and these defects may effectively contribute to the net degree of crystalline nature [35,36]. Note that XRD results have also shown the poor crystalline nature of the control sample. At the 1st shocked condition, the crystal surface turns into a highly smooth surface such that there is no visible signature for the planer and line defects for which the corresponding micrograph is depicted in Fig.8b. The reduction in line defects clearly demonstrates the formation of a homogeneous surface on the test sample during the shock wave loaded conditions and such changes may be due to the shock-wave induced dynamic recrystallization [49, 50]. After the second shocked condition, most part of the

crystal surface is smooth whereas there are uneven surfaces in a few parts of the crystal. After the 3rd shocked condition, the observed surface area of the crystal exhibits an uneven surface that may be due to the formation of an amorphous state and the corresponding micrograph is portrayed in Fig.8c and d. Surprisingly, at the 4th shocked condition, the uneven surface is turned into a flat surface and such morphological changes in the surface may be due to the amorphous to crystalline state phase transition such that the corresponding micrograph is presented in Fig.8e. Finally, after the 5th shocked condition, the surface of the test sample has some kind of a rough surface possessing a high density of surface defects, and the corresponding micrograph is depicted in Fig.8f. The observed high density surface defects contribute to the loss of a net degree of crystalline nature for the test sample.

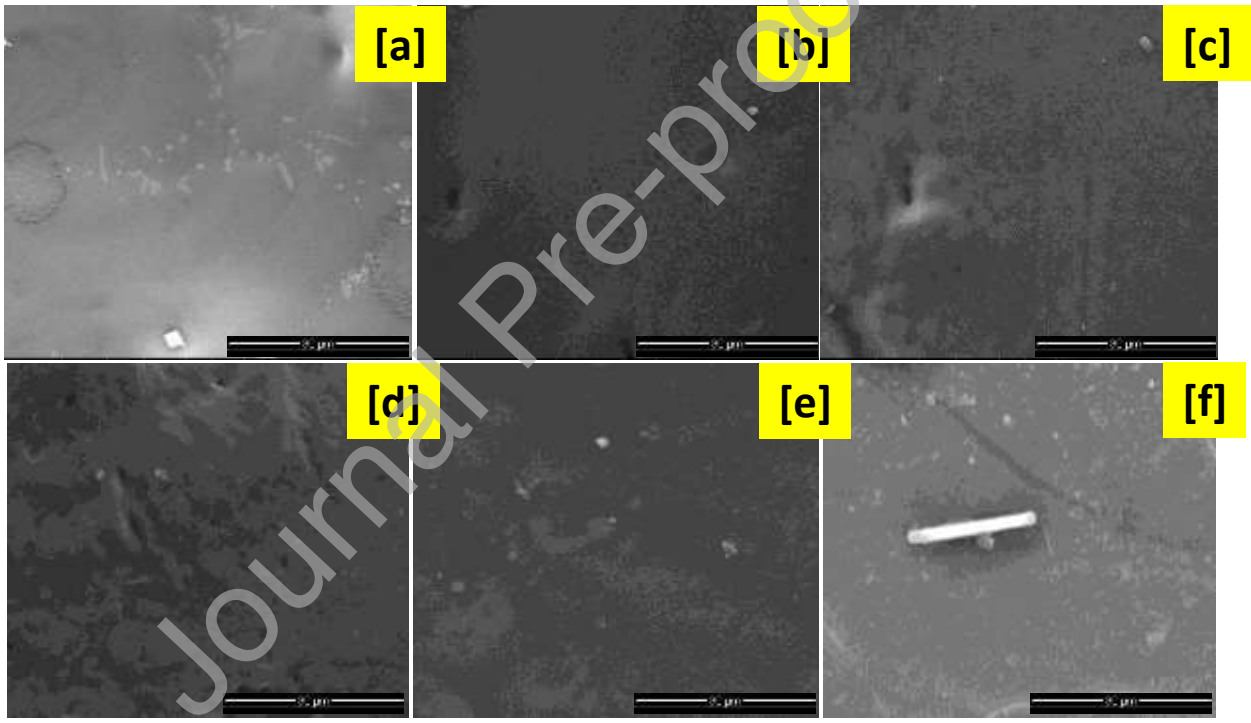

Fig.8 FE-SEM images of the control and shocked KNO_3 crystals (a) control (b)1st shocked (c)2nd shocked (d) 3rd shocked (e) 4th shocked (f) 5th shocked

Conclusion

In summary, the crystallographic phase stability of KNO_3 crystal (phase-II) is examined at shocked conditions with respect to different number of shock pulses, possessing the constant Mach number (1.7), such as 0,1,2,3,4 and 5, respectively and the results are successfully evaluated by X-

ray diffraction, Raman vibrational spectroscopy, optical spectroscopy and electron microscopic techniques. Based on the observed analytical results, the test crystal is proved to undergo the following phase transition sequence of crystal-crystal-crystal-amorphous-crystal-glassy crystalline nature for 0,1,2,3,4 and 5 shock pulses, respectively. As per the XRD and Raman results, the formation of crystal-amorphous-crystal phase transition is due to the occurrence of the rotational and positional disorder of the NO_3 groups. Moreover, the positional disorder of the K atoms and electronic spectral results are also suggested for the similar disorder to occur at shocked conditions. Based on the optical transmission spectra of the control and shocked crystals, the thermoelectric properties and dielectric properties give rise to the anomalous behaviour which may provide a perfect fit for the nonvolatile random access memory devices. It is worthwhile to mention here that a number of reports have been reported, to date, on KNO_3 phase transitions with respect to temperature and pressure but this is probably the first report on the switchable phase transitions of the sequence crystal-amorphous-crystal and hence the test crystal is highly favorable for the applications of molecular switches, nonvolatile random access memory devices.

Competing financial interests

The authors declare no competing financial interests.

Availability of Data

The data that support the findings of this study are available from the corresponding author upon reasonable request.

Compliance with ethical standards

None

Conflict of interest

The authors declare that they have no conflict of interest

Acknowledgment

The authors thank Department of Science and Technology (DST), India for DST-FIST progarmme (SR/FST/College-2017/130 (c)).

The project was supported by Researchers Supporting Project number (RSP-2021/231), King Saud University, Riyadh, Saudi Arabia.

References

[1] Lin Zhou, Ping-Ping Shi, Xuan Zheng, Fu-Juan Geng, Qiong Ye and Da-Wei Fu; Molecular design of high-temperature organic dielectric switches. Chem. Commun., 2018, 54, 13111. DOI: https://doi.org/10.1039/C8CC07311B

[2] Zhanning Liu, Lu Zhang and Daofeng Sun, Stimuli-responsive structural changes in metal–organic frameworks. Chem. Commun., 2020, 56, 9416-9432. DOI https://doi.org/10.1039/D0CC03197F

[3] Xuan Zheng, Ping-Ping Shi, Yang Lu, Lin Zhou, Ji-Xing Gao, Fu-Juan Geng, De-Hong Wu, Da-Wei Fu ORCID logo and Qiong Ye; Dielectric and nonlinear optical dual switching in an organic–inorganic hybrid relaxor $[(C_{H3)3}PC_{H2}OH][Cd(SCN)_3]$. Inorg. Chem. Front., 2017, 4, 1445-1450. DOI: https://doi.org/10.1039/C7QI00300E

[4] Wojciech Wełnic and Matthias Wuttig; Reversible switching in phase-change materials. Mater.Today, 2008, 11, 21-27 DOI: https://doi.org/10.1016/S1369-7021(08)70118-4

[5] Kosuke Usui, Mikinori Ando, Daisuke Yokogawa, and Stephan Irle; Understanding the On−Off Switching Mechanism in Cationic Tetravalent Group-V-Based Fluoride Molecular Sensors Using Orbital Analysis. J.Phys.Chem.A 2015, 119, 12693−12698. DOI: https://doi.org/10.1021/acs.jpcb.6b02298

[6] Ye Cao, Guangyu Qi, Laizhi Sui, Yue Shi, Ting Geng, Dianlong Zhao, Kai Wang, Kaijun Yuan, Guorong Wu, Guanjun Xiao, Siyu Lu, and Bo Zou; Pressure-Induced Emission Enhancements of Mn^{2+} - Doped Cesium Lead Chloride Perovskite Nanocrystals. ACS Materials Lett. 2020, 2, 381−388. DOI: https://doi.org/10.1021/acsmaterialslett.0c00033

[7] Wen Cui, Mingguang Yao, Dedi Liu, Quanjun Li, Ran Liu, Bo Zou, Tian Cui, and Bingbing Liu; Reversible Polymerization in Doped Fullerides Under Pressure: The Case

Of $C_{60}(Fe(C_5H_5)_2)_2$. J.Phys.Chem. B, 2012, 116, 2643−2650.
DOI: https://doi.org/10.1021/jp210712y

[8] R. Quesada Cabrera, A. Sella, E. Bailey, O. Leynaud, P.F. McMillan; High-pressure synthesis and structural behavior of sodium orthonitrate Na_3NO_4. J.Solid.State.Chem: 184, 2011, 915-920 DOI: https://doi.org/10.1016/j.jssc.2011.02.013

[9] V. Jayaram, K.P.J. Reddy; Experimental study of the effect of strong shock heated test gases with cubic zirconia. Adv. Mater. Lett. 2016, 7, 100-150.
DOI: https://doi.org/10.5185/amlett.2017.6379

[10] V. Jayaram, K.P.J. Reddy; Catalytic Effect of CeO_2-Stabilized ZrO_2 Ceramics with Strong Shock-Heated Mono- and Di-Atomic Gases. J.Am.Ceram.Soc., 2016, 99, 4128–4136. DOI: https://doi.org/10.1111/jace.14454

[11] Guanjun Xiao, Kai Wang, Li Zhu, Xiao Tan, Yuancun Qiao, Ke Yang, Yanming Ma, Bingbing Liu, Weitao Zheng, and Bo Zou; Pressure-Induced Reversible Phase Transformation in Nanostructured Bi_2Te_3 with Reduced Transition Pressure. J. Phys. Chem. C 2015, 119, 3843−3848. DOI: https://doi.org/10.1021/jp512565b

[12] N.V. Chandra Shekara,P.Ch. Sahua, M. Yousufa, K. Govinda Rajana, M. Rajagopalan; Structural stability and compressibility behaviour of dialuminides of cerium and gadolinium under high pressure. Solid.State.Commun, 1999, 111, 529–533. DOI: https://doi.org/10.1016/S0038-1098(99)00270-7

[13] Thomas D. Bennett, Petra Simoncic, Stephen A. Moggach, Fabia Gozzo, Piero Macchi, David A. Keen, Jin-Chong Tan and Anthony K. Cheetham; Reversible pressure-induced amorphization of a zeolitic imidazolate framework (ZIF-4). Chem. Commun., 2011, 47, 7983–7985. DOI: https://doi.org/10.1039/C1CC11985K

[14] Lingrui Wang, Tianji Ou, Kai Wang, Guanjun Xiao, Chunxiao Gao, and Bo Zou; Pressure-induced structural evolution, optical and electronic transitions of nontoxic organometal halide perovskite-based methylammonium tin chloride. Appl. Phys. Lett. 2017, 111, 233901. DOI: https://doi.org/10.1063/1.5004186

[15] Xiaoli Huang, Defang Duan, Kai Wang, Xinyi Yang, Shuqing Jiang, Wenbo Li, Fangfei Li, Qiang Zhou, Xilian Jin, Bo Zou, Bingbing Liu, and Tian Cui; Structural and Electronic Changes of $SnBr_4$ under High Pressure. J.Phys. Chem. C, 2013, 117, 8381−8387. DOI: https://doi.org/10.1021/jp310814k

[16] Xujie Lü, Qingyang Hu, Wenge Yang, Ligang Bai, Howard Sheng, Lin Wang, Fuqiang Huang, Jianguo Wen, Dean J. Miller, and Yusheng Zhao; Pressure-Induced Amorphization in Single-Crystal Ta_2O_5 Nanowires: A Kinetic Mechanism and Improved Electrical Conductivity. J. Am. Chem. Soc. 2013, 135, 13947–13953. DOI: https://doi.org/10.1021/ja407108u

[17] N. Koteeswara Reddy, V. Jayaram, E. Arunan, Y.-B. Kwon, W.J. Moon, K.P.J. Reddy, Investigations on high enthalpy shock wave exposed graphitic carbon nanoparticles. Diam. Relat. Mater. 2013, 35, 53–57A. DOI: http://dx.doi.org/10.1016/j.diamond.2013.03.005

[18] Tarak N. Maity, Nagarajan K. Gopinath, S. Janardhanraj, Krishanu Biswas, and Bikramjit Basu , Computational and Microstructural Stability Analysis of Shock Wave Interaction with NbB_2-B_4C-Based Nanostructured Ceramics. ACS Appl. Mater. Interfaces 2019, 11, 47491−47500. DOI: https://doi.org/10.1021/acsami.9b13995

[19] Xuan Zhou, Yu-Run Miao, William L. Shaw, Kenneth S. Suslick, and Dana D. Dlott; Shock Wave Energy Absorption in Metal−Organic Framework. J. Am. Chem. Soc. 2019, 141, 2220−2223 DOI: https://doi.org/10.1021/jacs.8b12905

[20] Zhi Su, William L. Shaw, Yu-Run Miao, Sizhu You, Dana D. Dlott, and Kenneth S. Suslick; Shock Wave Chemistry in a Metal−Organic Framework. J. Am. Chem. Soc. 2017, 139, 4619–4622 DOI: https://doi.org/10.1021/jacs.6b12956

[21] V.Mowlika, A.Sivakumar, S. A. Martin Britto Dhas, C. S. Naveen, A. R. Phani, R. Robert. Shock wave‑induced switchable magnetic phase transition behaviour of $ZnFe_2O_4$ ferrite nanoparticles. J.Nanostruct. Chem, 2020, 10, 203–209. DOI: https://doi.org/10.1007/s40097-020-00342-0

[22] A. Rita, A. Sivakumar, S. Sahaya Jude Dhas, and S. A. Martin Britto Dhas; Reversible magnetic phase transitions of MnO_2 nano rods by shock wave recovery experiments. J.Mater.Sci: Mater Electron. 2020, 31, 20360–20367. DOI: https://doi.org/10.1007/s40097-020-00342-0

[23] A. Sivakumar, S. Soundarya, S. Sahaya Jude Dhas, K. Kamala Bharathi, and S. A. Martin Britto Dhas; Shock Wave Driven Solid State Phase Transformation of Co_3O_4 to CoO Nanoparticles. J. Phys. Chem. C 2020, 124, 10755−10763. DOI: https://doi.org/10.1021/acs.jpcc.0c02146

[24] A. Sivakumar, S. Reena Devi, S. Sahaya Jude Dhas, R. Mohan Kumar, K. Kamala Bharathi, and S.A.Martin Britto Dhas; Switchable Phase Transformation (Orthorhombic−Hexagonal) of Potassium Sulfate Single Crystal at Ambient Temperature by Shock Waves. Cryst. Growth Des. 2020, 20, 7111–7119.
DOI: https://doi.org/10.1021/acs.cgd.0c00214

[25] Mengmeng Chen, Yuesong Shen, Shemin Zhu, Peiwen Li; Digital phase diagram and thermophysical properties of KNO_3-$NaNO_3$-$Ca(NO_3)_2$ ternary system for solar energy storage. Vacuum. 2017, 145, 225-233
DOI: https://doi.org/10.1016/j.vacuum.2017.09.003

[26] V.V.Deshpande, M.D. Karkhanavala and U.R.K. Rao; Phase transitions in potassium nitrate. J. Therm. Anal. Calorim. 1974, 6, 613—621.
DOI: https://doi.org/10.1007/BF01911781

[27] Marco A. Aquino-Olivos, Jean-Pierre E. Grolier, Stanislaw L. Randzio, Adriana J. Aguirre-Gutierrez, and Fernando Garca-Sanchez; Transitiometric Determination of the Phase Diagram of KNO_3 between (350 and 650) K and at Pressures up to 100 MPa. J. Chem. Eng. Data 2010, 55, 5497–5503. DOI: https://doi.org/10.1021/je100663y

[28] R. Benages-Vilau, T. Calvet and M.A. Cuevas-Diarte; Polymorphism, crystal growth, crystal morphology and solid-state miscibility of alkali nitrates. Crystallogr. Rev. 2014, 20, 25-55. DOI: https://doi.org/10.1080/0889311X.2013.838673

[29] Z. Iqbal, C.W. Christoe and F.J.Owens; Pressure Induced Phase Transition In Antiferroelectric KNO_3. Ferroelectrics, 1977, 16, 229-231
DOI: https://doi.org/10.1080/00150197708237165

[30] M.K. Teng, M. Balkanski and J.F. Mourey; Pressure Induced Ferroelectric Phase Transition In Potassium Nitrate; Solid. State. Commun , 1971, 9, 465—469
DOI: https://doi.org/10.1016/0038-1098(71)90323-1

[31] T.G.Worlton, D.L.Decker, J.D. Jorgensen and R. Kleb; Structure of High-Pressure KNO_3-IV. Physica B, 1986, 136, 503-506. DOI: https://doi.org/10.1016/S0378-4363(86)80128-0

[32] A. Sivakumar, S. Balachandar, S. A. Martin Britto Dhas; Measurement of "Shock Wave Parameters" in a Novel Table-Top Shock Tube Using Microphones. Hum. Fact. Mech. Eng. Defense. Safety. 2020, 4, 3. DOI: https://doi.org/10.1007/s41314-019-0033-5

[33] A.Sivakumar, S.Sahaya Jude Dhas, S.Balachandar, and S.A. Martin Britto Dhas; Effect of shock waves on structural and dielectric properties of ammonium dihydrogen phosphate crystal. Z. Kristallogr. 2019, 234, 557–567. DOI: https://doi.org/10.1515/zkri-2018-2159

[34] Jorg Rolfs, Rolf Lacmann, Stephan Kipp; Crystallization of potassium nitrate (KNO_3) in aqueous solution I. Growth kinetics of the pure system. J.Cryst. Growth, 1997, 171, 174-182. DOI: https://doi.org/10.1016/S0022-0248(96)00430-7

[35] M. Senthil Pandian, P. Ramasamy; Sodium sulfanilate dihydrate (SSDH) single crystals grown by conventional slow evaporation and Sankaranarayanan–Ramasamy (SR) method and its comparative characterization analysis. Mater.Chem.Phys 2012, 132, 1019–1028. DOI: https://doi.org/10.1016/j.matchemphys.2011.12.057

[36] M. Senthil Pandian, K. Boopathi, P. Ramasamy, G. Bhagavannarayana; The growth of benzophenone crystals by Sankaranarayanan–Ramasamy (SR) method and slow evaporation solution technique (SEST): A comparative investigation. Mater.Res,Bull, 2012, 47, 826–835. DOI: https://doi.org/10.1016/j.materresbull.2011.11.052

[37] A. Sivakumar, S. Sahaya jude dhas, S. Balachandar, and S.A. Martin Britto Dhas; Impact of Shock Waves on Molecular and Structural Response of Potassium Dihydrogen Phosphate Crystal. J.Elect.Mater 2019, 48, 7868–7873. DOI: https://doi.org/10.1007/s11664-019-07605-9

[38] Jing Zhang, Weiguo Li, Zhengxiao Guo; Static recrystallization and grain growth during annealing of an extruded Mg-Zn-Zr-Er magnesium alloy. J.Magnes.Alloy, 2013, 1, 31-38. DOI: https://doi.org/10.1016/j.jma.2013.02.012

[39] Yury Meshcheryakov , Alexandre Divakov, Natali Zhigacheva and Boris Barakhtin; Multiscale Deformation and Dynamic Recrystallization in Shock Deformed Aluminum Alloy. Mater.Sci.Forum. 2014, 794, 815-820. DOI: https://doi.org/10.4028/www.scientific.net/MSF.794-796.815

[40] Yu. I. Meshcheryakov, A. K. Divakov, S. A. Atroshenko, and N. S. Naumova; Effect of Velocity Nonuniformity on the Dynamic Recrystallization of Metals in Shock Waves. Tech.Phys. Lett, 2010, 36, 1125–1128. DOI: https://doi.org/10.1134/S1063785010120187

[41] H.M.Lu and J.R.Hardy; First-principles study of phase transitions in KNO_3. Phys.Rev.B. 1991, 44, 7215-7224. DOI: https://doi.org/10.1103/PhysRevB.44.7215

[42] J.K.Nimmo, B.W.Lucas; Conformation and orientation of NO_3 in α-phase of potassium nitrate. Nat.Phys 1972, 237, 61-63. DOI: https://doi.org/10.1038/physci237061a0

[43] Ramaswamy Murugan, Pei Jane Huang, Anil Ghule, Hua Chang; Studies on thermal hysteresis of KNO_3 by thermo-Raman spectroscopy. Thermochimica Acta 2000, 346, 83-90. DOI; https://doi.org/10.1016/S0040-6031(99)00364-0

[44] M. H. Brwker; Raman spectroscopic investigations of structural aspects of the different phases of lithium sodium and potassium nitrate. J.Phys.Chem.Solids. 1978, 39, 657-667. DOI: https://doi.org/10.1016/0022-3697(78)90181-6

[45] M. Hafez, I.S. Yahia and S. Taha; Study of the Diused Reflectance and Microstructure for the Phase Transformation of KNO_3. Acta Physica Polonica A 2015, 127, 734-740. DOI: https://doi.org/10.12693/APhysPolA.127.734

[46] K. S. Krishnan, A.C. Guha; The absorption spectra of nitrates and nitrates in relation to their photo-dissociation. Proc.Indian Acad. Sci.1934, 1, 242–249. DOI: Not found

[47] C. Ghosh and B.P.Varma; Optical properties of amorphous and crystalline Sb_2S_3 thin films. Thin Solid Films, 1979, 60, 61-65. DOI: https://doi.org/10.1016/0040-6090(79)90347-X

[48] C. Ghosh and B.P. Varma; Some optical properties of amorphous and crystalline antimony trisulphide thin films. Solid.State.Commun, 1979, 31, 683-686. DOI: https://doi.org/10.1016/0038-1098(79)90323-5

[49] Prashant Kumar, Jing Liu, Maithilee Motlag, Lei Tong, Yaowu Hu, Xinyu Huang, Arkamita Bandopadhyay, Swapan K. Pati, Lei Ye, Joseph Irudayaraj, and Gary J. Cheng; Laser Shock Tuning Dynamic Interlayer Coupling in Graphene− Boron Nitride Moiré Superlattices. Nano Lett. 2019, 19, 283−291. DOI: https://doi.org/10.1021/acs.nanolett.8b03895

[50] Shiteng Zhao, Bimal Kad, Christopher E. Wehrenberg, Bruce A. Remington, Eric N. Hahn, Karren L. More, and Marc A. Meyers; Generating gradient germanium nanostructures by shock-induced amorphization and crystallization. PNAS, 2017, 114, 9791-9796. DOI: https://doi.org/10.1073/pnas.1708853114